

Renormalized density-functional theory of nonuniform superfluid ^4He at zero temperature*

C. Ebner

*Department of Physics, The Ohio State University, Columbus, Ohio 43210
and Battelle Memorial Institute, Columbus, Ohio 43201*

W. F. Saam

Department of Physics, The Ohio State University, Columbus, Ohio 43210

(Received 25 November 1974)

A density-functional theory is constructed for nonuniform systems of superfluid ^4He at zero temperature. In calculations of the free-surface shape and tension it is found necessary to self-consistently renormalize the theory in order to account for the important effects of the zero-point motion of the long-wavelength (wave number $q \leq q_m$) surface modes. Use of a cutoff $q_m = 0.99 \text{ \AA}^{-1}$, self-consistently determined within the theory, yields a surface tension of 0.384 erg/cm^2 , which compares well with the experimental results of 0.378 erg/cm^2 . Detailed liquid-structure effects are included, but no static density oscillations near the free surface result, in contrast to a theory of Regge. When the theory is applied to the case of ^4He bounded by a single hard wall, density oscillations near the wall are obtained. For a much simplified version of the density functional, an analytic solution for a planar free surface, vortex-line structure, and various properties of ^4He droplets, including the curvature dependences of the surface tension and Gibbs surface mass, are obtained.

I. INTRODUCTION

In recent years a considerable amount of effort has been devoted to the study of many-body systems which possess some essential nonuniformity, the most extreme example being a surface separating two phases. One of the most widely used theoretical tools employed in such studies is density-functional (DF) theory. The physical ideas involved have been in existence at least as long as the Thomas-Fermi model of the atom, but their firm theoretical basis has been established only comparatively recently by Hohenberg and Kohn¹ and by Mermin.¹ Recently, the DF theory has been applied to problems as diverse as those associated with the electron density in the vicinity of metal surfaces,² liquid helium,^{3,4} nuclear matter,⁵ classical liquids,⁶ and self-trapped electron states in dense gases.⁷

While the DF theory is in principle exact,¹ in practice, the density functionals are always constructed using, in an essential way, the concept of local uniformity. This approximation is applied even when the nonuniformity is as extreme as the formation of a free surface, where the density may vary drastically over a distance of only a few atomic diameters. What may be essential new correlations introduced by the presence of the nonuniformity are incorrectly treated. This neglect turns out to be particularly important in a calculation of the free-surface tension and profile for zero-temperature ^4He . In this case the presence of the free surface radically alters the nature of the long-wavelength (i.e., longer than a few interatomic spacings) elementary excitation spectrum. What was a spectrum containing simply phonons in the case of a uniform system becomes one containing both exci-

tations localized near the surface (rippions) and phonons reflected at the surface.⁸ This change has two important consequences. The first is a considerable zero-point-motional broadening of the surface. The second is an important contribution to the surface energy arising from the zero-point energy of both the ripples and the surface-modified phonons. That the ripplon zero-point energy is important was recognized some years ago by Atkins.⁹ A somewhat similar point has been discussed concerning the electron contribution to the surface energy of metals¹⁰; however, there are significant qualitative differences between the ^4He and electron problems. Our treatment of ^4He incorporates these zero-point-motion effects via a renormalization of the density-functional results calculated in their absence.

In Sec. II we first develop a bare-density-functional (BDF) theory, "bare" in that zero-point-motion effects are not included. Subsequently, we present our prescription for renormalization. Section III is devoted to the details involved in calculating the input for the BDF theory: the energy density, liquid-structure factor, and nonlocal effective interaction as functions of ^4He density.

In Sec. IV we present our results. The nonlinear integro-differential equation determining the bare-density profile and, consequently, the surface tension is first solved. The renormalization procedure is then implemented. A self-consistent procedure for determining the mode wave-number cutoff $q_m = 0.99 \text{ \AA}^{-1}$ is developed, yielding a surface tension of 0.384 erg/cm^2 , in good agreement with the experimentally determined value of 0.378 erg/cm^2 . Other methods of determining q_m are also discussed. The surface density profile contains no

oscillations (neither does the bare profile), in contrast to results of a recent theory of Regge,¹¹ but in agreement with calculations, based on approximate wave functions, of Shih and Woo¹² and Chang and Cohen.¹³ In order to check that our theory is capable of producing oscillations (they result from hard-core effects), we apply it to the case where the liquid has not a free surface, but one bounded by a hard wall, and we find density oscillations similar to those found by Liu, Kalos, and Chester¹⁴ for a hard-sphere boson system bounded by two hard walls. This contrasting behavior shows that a free surface is simply too soft to permit static oscillations in the density.

In Sec. V we present results of a number of calculations based upon a simplified DF theory. This theory has the virtue that it possesses an analytic solution for the free-surface case. Further, it permits easy calculation of the density profiles near a vortex line and for small helium droplets. In the latter situation the curvature dependence of the surface tension and the Gibbs surface mass (quantities of interest in the recent work of Edwards, Eckhardt, and Gasparini¹⁵ concerning the surface excitation spectrum) are obtained for the first time.

In Sec. VI we present a discussion and summary of our results. A short discussion of ways in which the width characterizing the free-surface profile might be measured is given.

II. THEORETICAL FORMALISM

We begin this section with the development of what we term the bare-density-functional (BDF) theory. Our use of the adjective bare is to indicate that this formalism, as is the case with all previous such theories,^{3-5,10} fails to include the effect of zero-point motion of the surface. The reason for this failure is that BDF theories generally involve expansions about the uniform-system limit, and thus contain energies and response functions appropriate to a uniform system at an arbitrary density. Any information about changes in mode structure due to the formation of a surface is lost. The second portion of this section explains our method of modifying the BDF in order to include the changes in mode structure in a self-consistent way.

A. Bare-density-functional theory

The approach we take here is similar to that of Hohenberg and Kohn.¹ For the sake of completeness, and because of significant differences between the ⁴He problem and the electron problem treated by these authors, we go into some detail.

The basic assumption¹⁶ made is that the energy E of a nonuniform system of superfluid ⁴He at zero temperature may be uniquely expressed as a func-

tional of the number density n . We approximate this functional in terms of a local energy density plus an expansion in powers of the difference between densities at different points in the fluid; the series is terminated in second order. Thus,

$$E[n] = \int d^3r \epsilon(n(\vec{r})) + \int d^3r d^3r' \gamma(\vec{r}, \vec{r}') [n(\vec{r}) - n(\vec{r}')] + \int d^3r d^3r' W(\vec{r}, \vec{r}') [n(\vec{r}) - n(\vec{r}')]^2. \quad (2.1)$$

Here $\epsilon(n)$ is the energy density of a uniform system having density n . Further, symmetry requires that $\gamma(\vec{r}, \vec{r}')$ and $W(\vec{r}, \vec{r}')$ be even functions upon interchange of \vec{r} and \vec{r}' . Thus, (2.1) simplifies to

$$E[n] = \int d^3r \epsilon(n(\vec{r})) + \int d^3r d^3r' W(\vec{r}, \vec{r}') [n(\vec{r}) - n(\vec{r}')]^2. \quad (2.2)$$

The kernel $W(\vec{r}, \vec{r}')$ may be thought of as an effective interaction between different portions of the fluid arising because of nonuniformity.

Equation (2.1) is strictly correct for small variations in $n(\vec{r})$ around some average density n_0 ; $W(\vec{r}, \vec{r}')$ is then a function of n_0 and $\vec{r} - \vec{r}'$. In applications where $n(\vec{r})$ varies by a large amount and where there is no average density around which one can reasonably expand (e.g., the liquid surface), it is necessary to have some prescription for choosing the density \bar{n} at which W is to be evaluated. A simple, convenient, and intuitively appealing procedure which has the correct behavior in the uniform-system limit is to pick $\bar{n} = \frac{1}{2}[n(\vec{r}) + n(\vec{r}')]$; thus,

$$W(\vec{r}, \vec{r}') \rightarrow W\{\vec{r} - \vec{r}'; \frac{1}{2}[n(\vec{r}) + n(\vec{r}')] \}. \quad (2.3)$$

To obtain an explicit expression for W , we look at the case of a fluid perturbed only slightly from the average density n_0 . Then,

$$n(\vec{r}) = n_0 + \delta n(\vec{r}), \quad \int d^3r \delta n(\vec{r}) = 0. \quad (2.4)$$

Combination of (2.2)-(2.4) yields, to second order in δn

$$E[n] = E_0 + \frac{1}{2} \int d^3r \frac{\partial^2 \epsilon_0}{\partial n^2} [\delta n(\vec{r})]^2 + 2W_0 \int d^3r [\delta n(\vec{r})]^2 - 2 \int d^3r d^3r' W(\vec{r} - \vec{r}'; n_0) \delta n(\vec{r}) \delta n(\vec{r}'), \quad (2.5)$$

where E_0 and ϵ_0 are, respectively, the ground-state energy and ground-state-energy density of the system at density n_0 , and

$$W_0 \equiv \int d^3r W(\vec{r}; n_0). \quad (2.6)$$

Now, it is an exact result¹ of second-order perturbation theory that

$$E[n] = E_0 + \frac{1}{2} \int d^3r d^3r'$$

$$\times \left(\int \frac{d^3 q}{(2\pi)^3} e^{i\vec{q} \cdot (\vec{r} - \vec{r}')} \chi_q^{-1} \right) \delta n(\vec{r}) \delta n(\vec{r}'), \quad (2.7)$$

where χ_q is the retarded density-density response function at wave number \vec{q} for the uniform system. Comparison of (2.5) and (2.7), combined with the compressibility sum-rule result $\chi_{\vec{q}=0}^{-1} = \partial^2 \epsilon_0 / \partial n_0^2$,¹⁷ yields the identification

$$W(\vec{r} - \vec{r}'; n_0) = -\frac{1}{4} \int \frac{d^3 q}{(2\pi)^3} e^{i\vec{q} \cdot (\vec{r} - \vec{r}')} \chi_q^{-1}(n_0). \quad (2.8)$$

Consequently, (2.2) becomes

$$E[n] = \int d^3 r \epsilon(n(r)) - \frac{1}{4} \int d^3 r d^3 r' \times \left(\int \frac{d^3 q}{(2\pi)^3} \frac{e^{i\vec{q} \cdot (\vec{r} - \vec{r}')}}{\chi_q(\bar{n})} \right) [n(\vec{r}) - n(\vec{r}')]^2. \quad (2.9)$$

Now, in the limit that $\vec{q} \rightarrow \infty$, χ_q must approach the free-particle result

$$\chi_q^{0-1}(n) = \hbar^2 q^2 / 4mn, \quad (2.10)$$

in which m is the ⁴He atomic mass. The integral over wave numbers in (2.9) is thus irregular for large \vec{q} . It is convenient to separate out the free-particle limit in order to obtain a regular kernel, a procedure which yields, after some simple manipulations,

$$E[n] = \int d^3 r \epsilon(n(\vec{r})) + \frac{\hbar^2}{2m} \int d^3 r [\vec{\nabla} n^{1/2}(\vec{r})]^2$$

$$E[n] = \int_{-\infty}^{\infty} dz \epsilon(n(z)) + \frac{\hbar^2}{2m} \int_{-\infty}^{\infty} dz [n^{1/2'}(z)]^2 - \frac{1}{4} \int_{-\infty}^{\infty} dz \int_{-\infty}^{\infty} dz' \left[\int_{-\infty}^{\infty} \frac{dq}{2\pi} \frac{\hbar^2 q^2}{4m\bar{n}} \left(\frac{1}{S_q^2(\bar{n})} - 1 \right) e^{i q(z-z')} \right] [n(z) - n(z')]^2, \quad (2.13)$$

where a prime on a function denotes differentiation with respect to its argument. The equilibrium configuration assumed by the system is then the solution of

$$\delta E[n] / \delta n(z) = \mu, \quad (2.14)$$

subject to appropriate boundary conditions. Here μ is the chemical potential. For brevity, let

$$\Lambda(z - z') = \frac{\hbar^2}{4m\bar{n}} \int_{-\infty}^{\infty} \frac{dq}{2\pi} q^2 [S_q^{-2}(\bar{n}) - 1] e^{i q(z-z')}. \quad (2.15)$$

Written out explicitly, (2.14) as found from (2.13) and (2.15) is

$$-\frac{\hbar^2}{2m} \frac{n^{1/2''}(z)}{n^{1/2}(z)} + \epsilon'(n(z)) + \int_{-\infty}^{\infty} dz' \Lambda(z - z'; \bar{n}) [n(z) - n(z')] - \frac{1}{4} \int_{-\infty}^{\infty} dz' \frac{\partial \Lambda(z - z', \bar{n})}{\partial \bar{n}} [n(z) - n(z')]^2 = \mu. \quad (2.16)$$

It is this nonlinear integro-differential equation which we solve in Sec. III for the bare-surface-density profile associated with the free surface. For future reference, we point out that the surface tension associated with the solution $n_b(z)$ to (2.16) is²³

$$\sigma_b = E[n_b] - \int_{-\infty}^{\infty} dz \mu n_b(z). \quad (2.17)$$

$$-\frac{1}{4} \int d^3 r d^3 r' \left(\int \frac{d^3 q}{(2\pi)^3} e^{i\vec{q} \cdot (\vec{r} - \vec{r}')} \times [\chi_q^{-1}(\bar{n}) - \chi_q^{0-1}(\bar{n})] [n(\vec{r}) - n(\vec{r}')]^2 \right). \quad (2.11)$$

The term involving $\vec{\nabla} n^{1/2}(\vec{r})$ in (2.11) is the well-known quantum pressure term first used by Gross.¹⁸⁻²⁰ It is a very pleasing feature of the present theory that this term emerges in a completely natural fashion²¹ and does not have to be put in by hand as has been done in the essentially phenomenological theory of Padmore and Cole.⁴

In order to make practical use of (2.9) we require a reasonable approximation for χ_q . Our choice is to employ the result of the Feynman theory²²:

$$\chi_q^{-1} = \hbar^2 q^2 / 4m S_q^2 n, \quad (2.12)$$

where S_q is the usual liquid-structure factor. While this approximation is not the best theory of ⁴He, it does include the structure of the system in a very reasonable way. Further, it renders actual computation of χ_q as a function of density reasonably tractable.

With (2.12), and the assumption that variations in the system occur only in the z direction (e.g., only in the direction normal to a planar surface), (2.11) takes the form (for unit area normal to the z axis)

B. Inclusion of the surface modes

As discussed in Sec. I, in the neighborhood of a planar free surface of superfluid ⁴He, correlations differ drastically from those deep in the bulk. This effect is most manifest in the longer-wavelength elementary excitation spectrum, which contains both ripples and phonons reflected at the surface, rather than merely freely propagating phonons.

This alteration, which leads to both a zero-point-motional broadening of the surface and an additional contribution to the surface energy, has nowhere been accounted for in the above development. Changes in the very short-wavelength part of the spectrum are at least approximately dealt with via the density dependence of ϵ and S_q . We note that a theory yielding riplons and surface-reflected phonons is one which begins in zeroth order with a sharp surface,²⁴ whereas in practice density-functional theories embark from the uniform-system limit. The formalism to be described below unifies these two approaches in a self-consistent way.

We begin by noting that we may regard, after Gross¹⁸ and Pitaevski,²⁵ the BDF result (2.16) as a semiclassical equation determining a classical field $n_b(z)$. The small oscillations of the density are then, when quantized, the elementary excitations of the system. Our approach for including the effects of the zero-point motion associated with these excitation is made most clear by first considering the case where the liquid has a perfectly sharp surface at $z=0$, corresponding to a bare density $n_0\Theta(z)=n_0$ for $z>0$, 0 for $z<0$. The excitations will give rise to fluctuations in both the position of the surface and in the density below the surface. Consequently, the density operator becomes

$$n_{\text{tot}}^{\text{op}}(\vec{r}) = [n_0 + \delta n^{\text{op}}(\vec{r})]\Theta[z + \zeta(x, y)], \quad (2.18)$$

where $\zeta(x, y)$ is the surface displacement associated with the excitations and $\delta n^{\text{op}}(\vec{r})$ describes the density fluctuations below the surface. Now, the $n_b(z)$ which we calculate in Sec. IV is, from the point of view of all but the very shortest-wavelength excitations, a step function. For these excitations, then, the approximation

$$n_{\text{tot}}^{\text{op}}(\vec{r}) = [n_0 + \delta n^{\text{op}}(\vec{r})] \frac{n_b[z + \zeta(x, y)]}{n_0} \quad (2.19)$$

is a good one. Further, if renormalization of the density due to fluctuations in $\zeta(x, y)$ is the only important effect (a statement to be justified later) $n_{\text{tot}}^{\text{op}}(\vec{r})$ becomes

$$n_{\text{tot}}^{\text{op}}(\vec{r}) = n_b[z + \zeta(x, y)] \quad (2.20)$$

and the renormalized density is

$$n(z) = \langle 0 | n_b[z + \zeta(x, y)] | n \rangle, \quad (2.21)$$

where $|0\rangle$ is the excitation ground state. The operator $\zeta(x, y)$ has the form

$$\zeta(x, y) = \sum_{\vec{q}, l} e^{i\vec{q}\cdot\vec{r}} (\zeta_{\vec{q}, l}^* a_{\vec{q}, l}^\dagger + \zeta_{\vec{q}, l} a_{\vec{q}, l}), \quad (2.22)$$

in which \vec{q} is a wave vector parallel to the surface, l is an index referring to both surface and bulk modes, and $a_{\vec{q}, l}^\dagger$ creates an excitation characterized by \vec{q} and l . The normal mode amplitude $\zeta_{\vec{q}, l}$ will be computed from the linear theory of quantum hydrodynamics for an ideal compressible fluid with a free surface.

Inserting (2.22) in (2.21) gives

$$\begin{aligned} n(z) &= \int_{-\infty}^{\infty} \frac{dk}{2\pi} e^{ikz} n_{bk} \langle 0 | e^{ik\zeta(x, y)} | 0 \rangle \\ &= \int_{-\infty}^{\infty} \frac{dk}{2\pi} e^{ikz} n_{bk} e^{-k^2 \zeta_0^2 / 2}. \end{aligned} \quad (2.23)$$

Here, n_{bk} is the Fourier transform of $n_b(z)$,

$$\zeta_0^2 \equiv \langle 0 | \zeta^2(x, y) | 0 \rangle = \sum_{\vec{q}, l} |\zeta_{\vec{q}, l}|^2 \quad (2.24)$$

is the mean-square surface displacement, $|0\rangle$ is the ground state for the excitations, and we have made use of a well-known result²⁶ concerning expectation values of exponentials of operators of the form (2.22). The result (2.24) is easily put in the more convenient and transparent form

$$n(z, \sigma_b) = \int_{-\infty}^{\infty} dz' n_b(z - z') e^{-z'^2 / 2\zeta_0^2} (2\pi\zeta_0^2)^{-1/2}, \quad (2.25)$$

where we have explicitly noted that the density depends upon σ_b . The effect of the zero-point motion has been simply to fold the bare density with a Gaussian whose width is determined by the mean-square surface displacement ζ_0^2 . The quantum-hydrodynamic result for ζ_0^2 (obtained in the Appendix) is

$$\zeta_0^2 = \frac{\hbar}{\pi \rho S b^2} \left(0.196 + \frac{1}{4\pi} \int_0^{b^2 q_m^2} I(x) dx \right), \quad (2.26)$$

$$I(x) \equiv \frac{1}{2} \left[1 + \frac{x}{(1+x)^{3/2}} \ln \left(\frac{(1+x)^{1/2} + x^{1/2}}{(1+x)^{1/2} - x^{1/2}} \right) \right], \quad b = \frac{\sigma_b}{\rho S^2}.$$

Here, q_m is a high-wave-number cutoff which is self-consistently determined within our theory in Sec. IV.

Next, we obtain the contribution of the zero-point motion of the phonons and riplons to the surface tension. This is just the difference between the zero-point energy per unit area of the system with a free surface and that of an equivalent amount of bulk liquid, and is expressed as (from the Appendix) a sum of two terms

$$\sigma_{zp}(\sigma_b) = \sigma_{zp}^{\text{phonon}} + \sigma_{zp}^{\text{riplon}}, \quad (2.27)$$

where, assuming unit surface area,

$$\sigma_{zp}^{\text{riplon}} = \frac{2\sqrt{2}\hbar S}{\pi b^3} \int_0^{b^2 q_m^2} x^2 [-x^2 + x(1-x^2)^{1/2}]^{1/2} dx,$$

$$\sigma_{zp}^{\text{phonon}} = -\frac{\hbar S q_m^3}{48\pi} - \frac{\hbar S}{8\pi^2 b^3} \int_0^1 dx \frac{(1-x^2)(1-2x^2)}{f(x)} \left(b^2 q_m^2 - \frac{1}{f(x)} \ln[1 + b^2 q_m^2 f(x)] \right). \quad (2.28)$$

Here, $f(x) = x^2(1-x^2)^2$. Note that $\sigma_{zp}(\sigma_b)$ is a function of σ_b .

The surface tension in our theory now contains two contributions, the bare result (2.17) and the zero-point-motion piece σ_{zp} . If these are simply added to give

$$\sigma = E[n_b(z)] - \int_{-\infty}^{\infty} dz \mu n_b(z) + \sigma_{zp}(\sigma_b), \quad (2.29)$$

we have an expression for σ which is inconsistent for two reasons. First, the renormalization of the density due to fluctuations in ξ is not included and second, the surface tension σ_b determining the excitations and appearing in both $\sigma_{zp}(\sigma_b)$ and $n(z, \sigma_b)$ is not the total surface tension. To obtain a self-consistent expression for σ , one must include both the density renormalization and the fact that the excitations themselves are renormalized by their own zero-point energy. This objective is clearly accomplished by replacing σ_b in $\sigma_{zp}(\sigma_b)$ and $n(z, \sigma_b)$ by σ and replacing $n_b(z)$ in (2.29) by $n(z, \sigma)$. Thus, the final expression for the surface tension is

$$\sigma = E[n(z, \sigma)] - \int_{-\infty}^{\infty} dz \mu n(z, \sigma) + \sigma_{zp}(\sigma). \quad (2.30)$$

This result, together with (2.25)–(2.28), and the bare density $n_b(z)$ provides us with a set of equations from which both the renormalized surface tension σ and the renormalized surface profile $n(z, \sigma)$ may be found.

To conclude this section we discuss the question of corrections to (2.20). Clearly, what one would like to do is to take the expectation value of (2.19). The calculations involved present some difficulties. To see this, note that in a linear theory $\delta n^{\text{op}}(\vec{r})$ has the form

$$\delta n^{\text{op}}(\vec{r}) = \sum_{\vec{q}, l} (n_{-\vec{q}, l}^* a_{-\vec{q}, l}^\dagger + n_{\vec{q}, l} a_{\vec{q}, l}) e^{i\vec{q} \cdot \vec{r}}, \quad (2.31)$$

where the mode amplitudes $n_{\vec{q}, l}(z)$ are functions of z , the surface having been fixed at $z=0$. In (2.19), however, $n_b[z + \xi(x, y)]$ has the surface at $z = -\xi(x, y)$. Consequently, the simple insertion of (2.31) into (2.19) is a procedure devoid of real physical meaning. A plausible way to repair the theory is to replace the z 's in (2.31) by $z + \xi(x, y)$. This amounts to a highly nonlinear renormalization of $\delta n^{\text{op}}(\vec{r})$ due to the presence of surface motion, and the physical notion involved is that the density adjusts adiabatically to the surface motion. If this replacement is made, and the expectation value computed in the same way that led to (2.25), one obtains

$$\langle 0 | \delta n^{\text{op}}[x, y, z + \xi(x, y)] n_b[z + \xi(x, y)] | 0 \rangle / n_0$$

$$= -\frac{1}{\rho \xi_0^2} \int_{-\infty}^{\infty} dz' S_{\rho\xi}(z-z') z' n_b(z-z') \times e^{-z'^2/2\xi_0^2} (2\pi\xi_0^2)^{-1/2}, \quad (2.32)$$

where the density-surface structure function $S_{\rho\xi}(z)$ is defined by

$$S_{\rho\xi}(z) = m \langle 0 | \delta n_{\text{op}}(z) \xi | 0 \rangle. \quad (2.33)$$

Evaluation of $S_{\rho\xi}(z)$ yields²⁷

$$S_{\rho\xi}(z) = \frac{\hbar q_m^2}{4\pi S} b^{1/2} \int_0^1 dx \frac{x \kappa^{3/2}(x) e^{-\kappa(x)z}}{[1 + (\frac{1}{2} b q_m x)^2]^{1/2}} - \frac{\hbar q_m^3}{2\pi^2 S} \frac{2 - 2 \cos q_m z - q_m z \sin q_m z}{(q_m z)^3}, \quad (2.34)$$

in which $\kappa(x) \equiv x q_m \{-\frac{1}{2} b q_m x + [1 + (\frac{1}{2} b q_m x)^2]^{1/2}\}$.

It is seen from Fig. 1 that $S_{\rho\xi}(z)$ contains considerable structure. Nevertheless, when (2.30) is solved, corrections to σ and $n(z, \sigma)$ due to including (2.32) amount to only a few percent, all of the structure in $S_{\rho\xi}(z)$ being washed out by the integration in (2.32).

In addition to density-fluctuation effects of the type given in (2.32), there are higher-order effects. For example, there will be a nonlinear correction to the $\delta n^{\text{op}}(\vec{r})$ of (2.31) coming from what is essentially the difference between the zero-point-motion "thermal expansion" in the uniform system and that in the system with a surface. While this cannot be calculated exactly without solving a nonlinear quan-

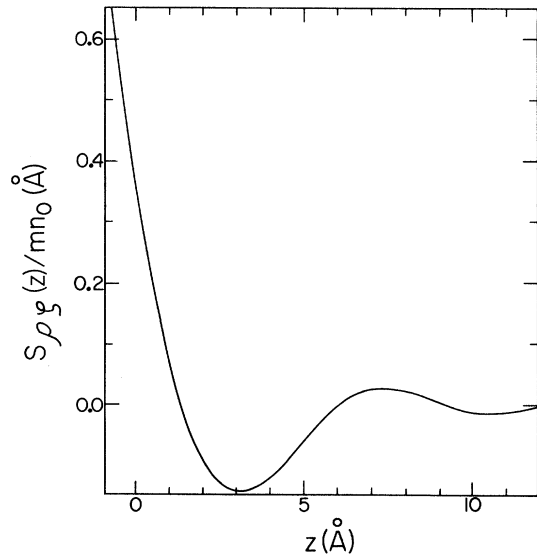


FIG. 1. Density-surface structure factor $S_{\rho\xi}(z)/m n_0$ as a function of z .

tum-hydrodynamics problem, detailed investigation²⁸ shows that the corrections have the same qualitative structure as those given in (2.32)–(2.34). Since these latter corrections have essentially no effect on the final density, there is no reason to believe that the former will. The physical reason for this is that the zero-point smearing of $n_b(z)$ caused by fluctuations in ζ is so large that any structure of the type given in (2.34) is washed out.²⁹

III. STRUCTURE FACTORS, ENERGY DENSITY, AND KERNELS

In order to obtain the bare-surface density from (2.16), it is first necessary to know the structure factor $S_q(n)$ and the energy density $\epsilon(n)$ in the uniform liquid. To obtain these we employ the theory of Mihara and Puff,³⁰ who derive the following two equations for the structure factor [Eq. (3.1) of Ref. 30] and for the energy density [Eq. (1.6) of Ref. 30] of the uniform liquid at $T=0$:

$$1/S_q^2(n) = 1 + 4nmV(q)/\hbar^2q^2 + (4m/\hbar^2q^4) \int d^3q'/(2\pi)^3 \times \{V(|\vec{q} + \vec{q}'|)[\hat{q} \cdot (\vec{q} + \vec{q}')]^2 - V(q')[\hat{q} \cdot \vec{q}']^2\} [S_{q'}(n) - 1] \quad (3.1)$$

and

$$\frac{d\epsilon(n)}{dn} = \frac{5}{3}\epsilon(n)/n + \frac{1}{8}nV(q=0) + \frac{1}{3} \int \frac{d^3q}{(2\pi)^3} [\frac{1}{2}\nabla_q^2(\vec{q}V(q)) - V(q)] [S_q(n) - 1]. \quad (3.2)$$

Here, $V(q)$ is a Fourier component of the interatomic potential $V(r)$,

$$V(q) = \int d^3r V(r) e^{-i\vec{q}\cdot\vec{r}} \quad (3.3)$$

and \hat{q} is a unit vector in the direction of \vec{q} . Although $V(r)$ is assumed to have a Fourier transform, this is not essential for the application of (3.1) and (3.2) since the integrals may also be formulated in terms of $V(r)$ and the radial distribution function $g_n(r)$ which is given by

$$g_n(r) = 1 + \frac{1}{n} \int \frac{d^3q}{(2\pi)^3} [S_q(n) - 1] e^{i\vec{q}\cdot\vec{r}}. \quad (3.4)$$

It is, however, more convenient to work with $V(q)$ and $S_q(n)$ when solving (3.1) in particular.

The potential we employ is the same as the one used in Ref. 30:

$$V(r) = E_0(a/r) (e^{-r/a} - \gamma e^{-\beta r/a}), \quad (3.5)$$

with $E_0 = 8.95 \times 10^5$ K, $\gamma = 0.2560$, $\beta = 0.8000$, and $a = 0.376$. In Fig. 2 this potential is compared with the more standard Lennard-Jones (6-12) potential for helium atoms

$$V_{LJ}(r) = 4V_0[(\alpha/r)^{12} - (\alpha/r)^6], \quad (3.6)$$

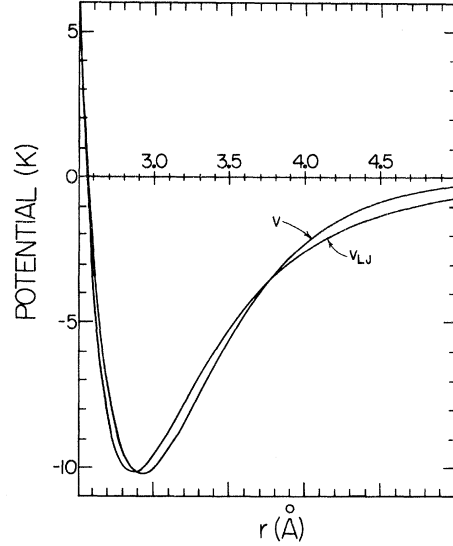


FIG. 2. Comparison of $V_{LJ}(r)$ and $V(r)$ as functions of r .

where $V_0 = 10.2$ K and $\alpha = 2.556$ Å. The two differ principally in the core region where $V(r)$ is softer than $V_{LJ}(r)$ and in the long-range attractive region where (3.5) approaches zero more rapidly than (3.6). The first of these differences should have an effect only on calculations done for very high density; we do not believe that the results presented below would be significantly altered by using, e.g., $V_{LJ}(r)$ rather than (3.5). As for the fact that $V(r)$ does not have the correct $1/r^6$ long-range behavior, it seems likely that this is partly responsible for the rather small discrepancies between the equilibrium energy and density found below and their experimental values. However, the difference between calculated and measured values is sufficiently small that $V(r)$ from (3.5) should be quite adequate for our purposes.

Our first task is to find $S_q(n)$ from (3.1) at a number of different densities using the Fourier transform of (3.5):

$$V(q) = 4\pi E_0 a^3 [1/(1 + q^2 a^2) - \gamma/(\beta^2 + q^2 a^2)]. \quad (3.7)$$

Substitution of (3.7) into (3.1) produces the equation that must be solved. A solution to this very equation has been presented by Mihara and Puff³⁰ for density $n \sim n_0$ where n_0 is the ^4He density at $T=0$ and $P=0$. Their procedure is described by Mihara³¹ who presents a detailed discussion of the properties of (3.1). In the present work we have followed their numerical procedure quite closely and have obtained $S_q(n)$ at 70 different values of n between 0 and $1.41n_0$. The basic idea is to make an initial guess for $S_q(n)$, insert this in the right-hand side of (3.1), and do the integral over q' to find a new $S_q(n)$. In the simplest iteration scheme,

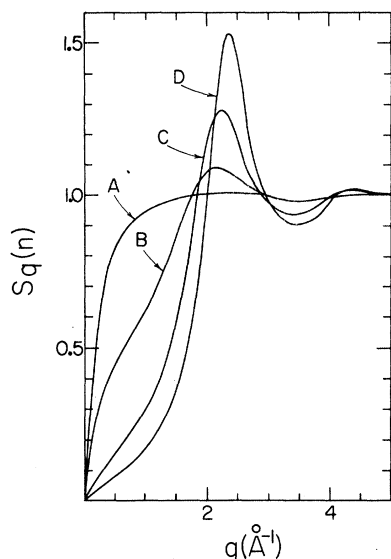


FIG. 3. Structure factors $S_q(n)$ as functions of q for n/n_0 equal to 0.1 (A), 0.5 (B), 1.0 (C), and 1.4 (D).

the new structure factor would in turn be used to produce another one and the procedure repeated until convergence is achieved. It turns out, however, that this method does not work; rather, it is necessary to use a weighted average of the result of previous iterations in order to obtain convergence. The convergence is examined by looking (at all q) at the difference between a given calculated structure factor and the one that is used to produce it. In practice it proved possible to obtain a maximum difference of less than 0.001 by using some 2000 iterations. For densities larger than about $0.8n_0$, the iteration procedure was terminated when the maximum difference between succeeding structure factors became smaller than 0.001; at smaller densities, the maximum difference was required to be smaller than 0.01.

Results for $S_q(n)$ at several representative densities are shown in Fig. 3; for $n \approx n_0$ (curve C), the calculated structure factor has a shape very close to the experimental one, consistent with the results presented in Refs. 30 and 31. The first peak becomes more pronounced as the density increases and moves to slightly larger q , behavior that is expected and supported by neutron scattering data.³² Further, for $n \sim n_0$ there is a distinct shoulder in S_q around $q = 0.5 \text{ \AA}^{-1}$, which is also observed experimentally. The oscillations in $S_q(n) - 1$ gradually die away as n is decreased and disappear altogether for $n \sim 0.1n_0$. Thus, we find structure factors that at the very least, contain all of the expected qualitative features of $S_q(n)$ for liquid helium and that are in rather good quantitative agreement with the measured structure factors at densi-

ties close to n_0 .

The energy density $\epsilon(n)$ is found by numerically solving (3.2); we first transform the integral to one in real space so that the equation is

$$\frac{d\epsilon(n)}{dn} = \frac{5}{3}\epsilon(n)/n - \frac{1}{3}n \int d^3r g_n(r) \left[\frac{1}{2} \vec{r} \cdot \vec{\nabla} V(r) + V(r) \right]. \quad (3.8)$$

The reason for reformulating the integral in real space is that a small error in $S_q(n)$ at large q can have a rather sizable effect on $\epsilon(n)$ as found from (3.2). To avoid this difficulty we first Fourier transform $S_q(n) - 1$ to find $g_n(r)$ and then find $\epsilon(n)$ from (3.8). Now, the error in $S_q(n)$ at large q will of course also lead to appreciable errors in $g_n(r)$, but these will be principally at small r ; at larger r , the factor $e^{i\vec{q}\cdot\vec{r}}$ in (3.4) oscillates rapidly for large q and thereby strongly reduces the effect of errors in the tail of the structure factor. On the other hand, since we know on physical grounds that $g_n(r)$ is essentially zero at small r ($r \lesssim 2.2 \text{ \AA}$), we can simply set it equal to zero in this region. Specifically, our procedure has been to use the Fourier transform of $S_q(n) - 1$ down to that value of r for which the computed radial distribution function first goes to zero and to then set $g_n(r) \equiv 0$ for all smaller r . In this way we believe that we have minimized the effect of numerical inaccuracy in the large q part of $S_q(n)$.

The results for the radial distribution function at several representative densities (the same densities as in Fig. 3) are shown in Fig. 4. These functions rise rapidly from zero to a peak value which increases and moves to smaller r as the density

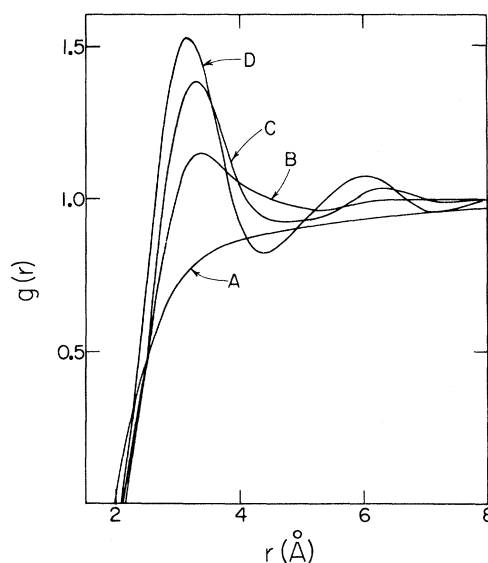


FIG. 4. Radial distribution functions $g_n(r)$ as functions of r for n/n_0 equal to 0.1 (A), 0.5 (B), 1.0 (C), and 1.4 (D).

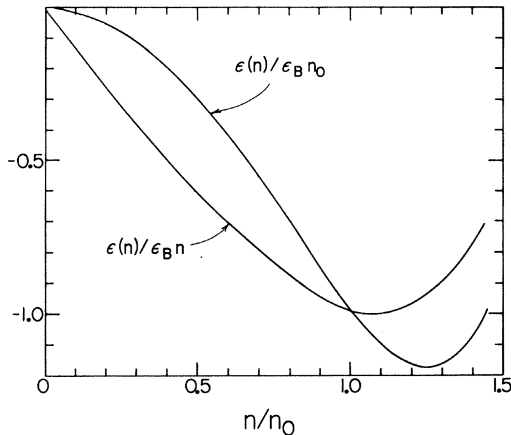


FIG. 5. Energy density and energy per particle as functions of number density.

increases. Following this peak is a train of decaying oscillations about unity. Thus, the computed $g_n(r)$ contain all of the expected qualitative features.

Given these functions, it is easy to do the integrals in (3.8) at various densities and to solve this first-order differential equation for $\epsilon(n)$. There is, however, one point that requires some discussion. Since (3.8) is a first-order differential equation, it is necessary to supply a boundary condition on the solution $\epsilon(n)$. This can be done in a variety of physically reasonable ways which need not all produce the same energy density because the formalism is not exact. For example, some reasonable boundary conditions are (i) that the calculated equilibrium density at $P=0$ be n_0 , (ii) that the energy per particle at $P=0$ be the ^4He chemical potential (-7.17 K) at zero temperature and pressure, and (iii) that the compressibility at $P=0$ be the experimental compressibility. Yet another condition, employed in Ref. 30, is (iv) that the $P=0$ compressibility found by computing $d^2\epsilon/dn^2$ be the same as that inferred from the slope of $S_q(n)$ for $q \rightarrow 0$. We have chosen to use the second boundary condition (ii) above. With this choice the calculated equilibrium density is found to be $1.08n_0$ or $2.36 \times 10^{22} \text{ cm}^{-3}$; by contrast we find that condition (iii) leads to an equilibrium density of $1.047n_0$ while (i) obviously gives n_0 . Mihara and Puff arrive at a density of about $1.045n_0$ using the fourth boundary condition. The spread in these results gives some idea of the validity and accuracy of the calculations. At least part of the spread is probably a consequence of the fact that the potential (3.5) falls off too rapidly at large r relative to the true interaction between helium atoms.

This property would tend to make the calculated equilibrium density larger than n_0 for most choices of the boundary condition. On the other hand, if the equilibrium density is forced to be n_0 as in con-

dition (i), then we would expect the energy per particle at this density to come out too high because the potential is not sufficiently attractive. This turns out to be the case: Condition (i) gives an energy some $2\frac{1}{2}$ K too high at $n=n_0$.

In Fig. 5 we plot the energy density and energy per particle as functions of the number density. Boundary condition (ii) was used in obtaining these functions, and it is this energy density that will be used in the calculations of the density at a planar surface in Sec. IV.

We consider next the determination of the kernel $\Lambda(z;n)$. In principle, it may be found from (2.15) by direct integration, but this integral is very sensitive to small deviations of $S_q(n)$ from unity at large q when z is small. We therefore adopt the same sort of procedure as that used in connection with the integral in (3.2). First, replace the factor $1/S_q^2(n)$ in (2.15) with the right-hand side of (3.1). Then write V and S as Fourier transforms and complete as many integrals as possible analytically. After some manipulation, the expression for the kernel becomes

$$\Lambda(z;n) = \pi \int_z^\infty r^3 dr g_n(r) \left\{ \left[1 - \frac{4}{3} \frac{z}{r} + \frac{1}{3} \left(\frac{z}{r} \right)^4 \right] \frac{d^2 V(r)}{dr^2} + \left[1 - \frac{8}{3} \frac{z}{r} + 2 \left(\frac{z}{r} \right)^2 - \frac{1}{3} \left(\frac{z}{r} \right)^4 \right] \frac{1}{r} \frac{dV(r)}{dr} \right\}. \quad (3.9)$$

Numerical evaluation of this integral is straightforward. The resulting kernels at several densities are shown in Fig. 6. At all densities $\Lambda(z;n)$ has the same qualitative behavior; starting from a positive value at $z=0$, it decreases very nearly linearly with z and becomes negative at $z \approx 2.6 \text{ \AA}$. There follows a shallow minimum at about 2.6 \AA and a long negative tail. The negative region is

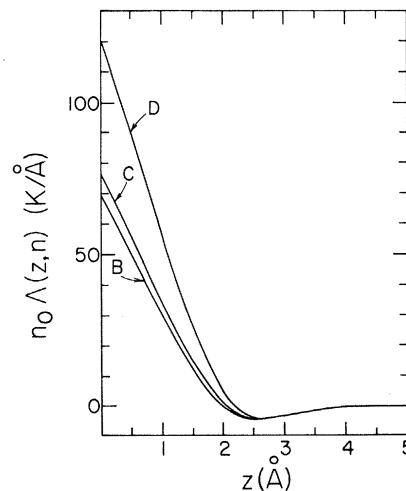


FIG. 6. The kernel $n_0 \Lambda(z;n)$ as a function of z for n/n_0 equal to 0.5 (B), 1.0 (C), and 1.4 (D).

quite insensitive to the density, while the short-range positive part of the kernel depends on n rather strongly for $n \sim n_0$ in particular, where it increases with increasing density. It is perhaps worth remarking that if $\Lambda(z;n)$ is evaluated directly from (2.15), the result for $z \gtrsim 2 \text{ \AA}$ is very nearly the same as when it is evaluated from (3.9). At smaller z , (2.15) gives a smaller kernel with a somewhat different shape. The discrepancy is a consequence of small errors in $S_q(n)$ at large q . The effect of these errors is reduced by using (3.9) and $g_n(r)$ computed in the manner described above. We note that Mihara³¹ was also aware of

this difficulty in evaluating other similar integrals over $S_q(n)$ and that he too chose to reformulate them as integrals over $g_n(r)$.

IV. RESULTS

A. Determination of $n_b(z)$

The bare density at a free planar surface of ^4He is found by solving (2.16) with $\epsilon(n)$ and $\Lambda(z;n)$ as determined in Sec. III. To this end we first write (2.16) in the form

$$n_b^{1/2''}(z) = B(z)n_b^{1/2}(z), \quad (4.1)$$

with

$$B(z) \equiv \frac{2m}{\hbar^2} \left\{ -\mu + \epsilon'(n_b(z)) + \int_{-\infty}^{\infty} dz' \Lambda(z-z';\bar{n}) [n_b(z) - n_b(z')] - \frac{1}{4} \int_{-\infty}^{\infty} dz' \frac{\partial \Lambda(z-z';\bar{n})}{\partial \bar{n}} [n_b(z) - n_b(z')]^2 \right\}, \quad (4.2)$$

where $\bar{n} = \frac{1}{2}[n_b(z) + n_b(z')]$ as in Sec. II. The boundary conditions on $n_b(z)$ are that $n_b(z) \rightarrow 0$ as $z \rightarrow -\infty$ and $n_b(z) \rightarrow n_\infty$ as $z \rightarrow \infty$; n_∞ is such that $-\mu + \epsilon'(n_\infty) = 0$ and depends on the boundary condition used in solving (3.2) for the energy density of the uniform system. As discussed in Sec. III, this condition was chosen to give the correct energy per particle or chemical potential at zero pressure. The corresponding equilibrium density is n_∞ and came out to be $1.08n_4$.

Our method of solving (4.1) and (4.2) is first, to choose some trial density to compute $B(z)$, and then to solve (4.1) by numerical integration, starting from the vacuum ($z \rightarrow -\infty$) side of the surface. The new density obtained in this last step is used to find $B(z)$ again and the procedure is repeated until convergence is obtained. There is a difficulty in that for arbitrary $B(z)$ the solution of (4.1) for the density does not necessarily approach n_∞ at large z . Therefore, the solution is truncated at some appropriate value of z , and a properly behaved tail, which goes to n_∞ as $z \rightarrow \infty$, is added. This function is then used to compute the next $B(z)$. After some effort we succeeded in obtaining a self-consistent solution to (4.1) and (4.2) which converged to n_∞ of its own accord.

To check on the validity of this result, we also found $n_b(z)$ variationally by constructing a parametrized analytic expression for the density and then minimizing the free energy per unit area,

$$F[n_b] = E[n_b] - \mu \int_{-\infty}^{\infty} dz n_b(z), \quad (4.3)$$

where (2.13) is used for $E[n_b]$. The density arrived at using this approach is essentially the same as that determined by direct solution of the integro-differential equation given the restrictions imposed

by the form of the variational trial function.

The bare density is plotted as a function of z in Fig. 7. It is a monotonic function of z with a very small width; defining the width Δz of the surface to be the distance between the points where $n_b = 0.1n_\infty$ and $0.9n_\infty$, we have for the bare surface $\Delta z_b = 0.64 \text{ \AA}$; this is much smaller than the widths obtained for the real ^4He surface in other theories.^{12,13} The free energy per unit area in (4.3), which is the same as the surface tension, comes out to be $\sigma_b = 0.003 \text{ erg/cm}^2$, much smaller than the $T=0$ experimental value¹⁵ of $\sigma_4 = 0.378 \text{ erg/cm}^2$.

These discrepancies in the density and surface tension are a consequence of having omitted zero-point-motion contributions as discussed in Sec. II. We turn next to consideration of the changes wrought by including these contributions and find, in particular, that they produce a sizable increase in both the surface tension and the surface width.

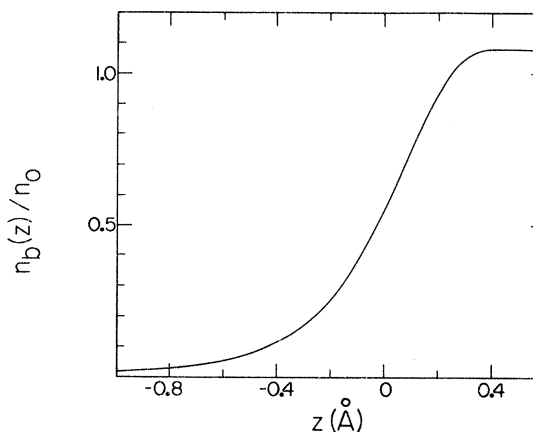


FIG. 7. Bare density $n_b(z)/n_0$ as a function of z .

B. Inclusion of surface zero-point-motion

Surface zero-point motion is accounted for *via* the formalism of Sec. II B. The numerical procedure is to start from some guess for σ , calculate ξ_0^2 , $n(z)$, and σ_{zp} from (2.26), (2.25), and (2.28), and then find a new value of σ from (2.30). These computations are repeated until the surface tension and the renormalized density $n(z)$ converge.

In order to carry out these manipulations, one must first make a choice of q_m . Our procedure is to relate q_m to the surface width, which is essentially $2\xi_0$ since the bare surface is very sharp, by the statement $q_m\xi_0(q_m) = \gamma$, where γ is a constant of order π . Now, for $q_m \sim 1 \text{ \AA}^{-1}$, ξ_0 is a decreasing function of q_m ; the reason is that an increase of the cutoff increases σ which makes the surface more rigid for high-wave-number ripples in a compressible fluid. As a consequence, $q_m\xi_0(q_m)$ exhibits a maximum at $q_m = 0.99 \text{ \AA}^{-1}$; the value at the maximum is 3.28. Hence, we cannot choose γ larger than 3.28 and, if we have $\gamma < 3.28$, the equations $q_m\xi_0(q_m) = \gamma$ and (2.30) do not possess a unique solution. Therefore we have chosen to use $\gamma = 3.28$ with the corresponding $q_m = 0.99 \text{ \AA}^{-1}$. This choice leads to $\sigma = 0.384 \text{ erg/cm}^2$, which compares very well with the experimental surface tension of 0.378 erg/cm^2 . In Fig. 8, the renormalized surface-density profile $n(z)$ is plotted. The surface width is $\Delta z = 7.8 \text{ \AA}$, larger than predicted by Shih and Woo¹² ($\approx 3 \text{ \AA}$) or by Chang and Cohen¹³ ($\approx 6 \text{ \AA}$). A discussion of possible experimental determinations of Δz is given in Sec. VI.

Other choices of q_m will naturally lead to different predictions of σ and $n(z)$. It turns out that the density profile is quite insensitive to the cutoff; for $0.95 \leq q_m \leq 1.05 \text{ \AA}^{-1}$, $n(z)$ deviates at most by $.02n_0$ from the curve shown in Fig. 8. The surface tension, on the other hand, varies from 0.369

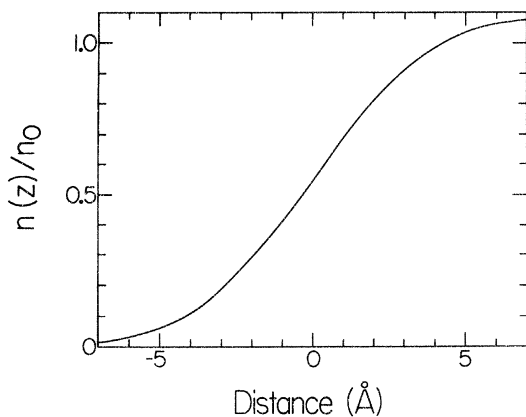


FIG. 8. Renormalized surface-density profile $n(z)/n_0$ as a function of z for $q_m = 0.99 \text{ \AA}^{-1}$.

at the smaller cutoff to 0.414 erg/cm^2 at the larger one. We believe that our choice of q_m is preferable to other ones because it is self-consistently determined within our theoretical framework. Nevertheless, it is possible to make other physically motivated selections of this number. For example, one could use the requirement that the imaginary part of the ripplon frequency be equal to the real part at $q = q_m$: $\text{Im}\omega_{q_m}^r / \text{Re}\omega_{q_m}^r = 1$. Ripplon damping has been calculated by Saam³³; using his results we find that this criterion implies $q_m = 0.973 \text{ \AA}^{-1}$ and $\sigma = 0.379 \text{ erg/cm}^2$. These numbers are very close to what we found above using an entirely different specification for the cutoff. One may also consider having different cutoffs q_m^r and q_m^p for the ripples and phonons. A simple way of picking these is to use the Debye model and count modes in two and three dimensions. Then, $q_m^r = \sqrt{8\pi} n_0^{1/3} = 1.395 \text{ \AA}^{-1}$ and $q_m^p = (18\pi^2 n_0)^{1/3} = 1.568 \text{ \AA}^{-1}$; the attendant value of σ is 0.429 erg/cm^2 . One would expect an overestimate since, for example, the bulk excitation spectrum ceases to be linear near $q \sim 0.8 \text{ \AA}^{-1}$.

Both the bare-surface profile $n_b(z)$ and the renormalized one $n(z, \sigma)$ are monotonically increasing functions of z , displaying no oscillations. This is in contradiction to the result of Regge,¹¹ who obtained significant oscillations. Regge's theory, which may be viewed as a rather rudimentary version of BDF theory, should in fact be compared with our unrenormalized theory. Even if a bare profile does contain oscillations, they will be washed out when the zero-point motion of the surface is included. The free surface is simply too soft to sustain static density oscillations (in contrast to the hard wall case to be discussed below). This conclusion is supported by calculations, based on the use of approximate wave functions, performed by Chang and Cohen.¹³ However, these authors used a scheme in which the surface energy was minimized via variation of only a few parameters in a trial function describing the surface profile. A similar calculation by Shih and Woo¹² involves a single-parameter fit which entirely rules out oscillations. Many parameters are needed to investigate oscillatory behavior (see our discussion of the hard wall case below). In fact, our solution of (2.16) is equivalent to an infinite-parameter minimization.

We have also investigated the renormalized density and surface tension by including (2.32) as a correction to (2.25), that is, (2.25) is replaced by

$$n(z, \sigma) = \int_{-\infty}^{\infty} dz' n_b(z - z') \left[1 - \frac{z'}{\rho \xi_0^2} S_{\rho \xi}^2(z - z') \right] \times e^{-z'^2/2\rho^2} (2\pi\xi_0^2)^{-1/2}. \quad (4.4)$$

The iterative procedure described above is used to

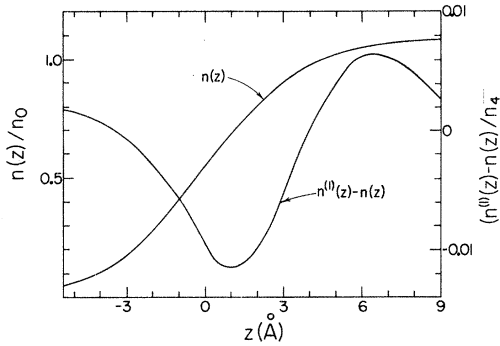


FIG. 9. Comparison of the renormalized density keeping zero-order and first-order terms in $\delta n^{\text{op}}(z)$ for $q_m = 1.0 \text{ \AA}^{-1}$.

find σ and $n(z)$. Although $S_{\rho\epsilon}$ is an oscillatory function, capable in principle of producing similar behavior in $n(z)$ even when $n_b(z)$ is monotonic, we find that no such behavior appears in the renormalized density because ζ_0 is comparable to the period of the oscillations in $S_{\rho\epsilon}$ and they are washed out by the integration over z' in (4.4). Indeed, the net effect of using this equation in place of (2.25) is small. Figure 9 compares the densities obtained in the two cases for a cutoff of $q_m = 1.0 \text{ \AA}^{-1}$; here, the density arising from (4.4) is denoted $n^{(1)}(z)$. The surface tension is also only slightly affected, being increased by about 1% when (4.4) is employed. Thus, we find that the net effect on $n(z)$ and σ of keeping first-order terms in $\delta n^{\text{op}}(\vec{r})$ is small, leading us to believe that higher-order corrections are unimportant.²⁸

C. Hard wall

We have also calculated the density $n_w(z)$ in the vicinity of a hard wall using the formalism of Sec. II A. The wall is assumed to be planar and located at $z=0$. The boundary conditions on $n_w(z)$ are $n_w(0)=0$ and $n_w(z) \rightarrow n_P$ as $z \rightarrow \infty$, where n_P is a constant determined by the pressure P which is applied to hold the liquid against the wall. For this case, severe convergence difficulties were encountered in attempting to solve the integro-differential equation for $n_w(z)$ by the method described in Sec. IV A, consequently, we have used the (in principle equivalent) procedure of minimizing $\sigma_{\text{wall}} = E[n_w] - \int_0^\infty dz \times [\mu n_w(z) - P]$ with respect to variations in $n_w(z)$. The trial density profile employed has the form

$$n_w(z) = n_P \left[1 - \left(1 + \sum_{j=1}^N \alpha_j z^j \right) e^{-\beta z^2} \right]^2, \quad (4.5)$$

where the α_j and β are varied. In Fig. 10 we show the result using ten parameters at a pressure of 24.4 atm. For smaller pressures, the size of the density oscillations decreases, as is to be expected. For the hard wall, our renormalization procedure

gives no corrections to this density profile since the surface is not free to move. The surface energy per unit area is then just the sum of $\sigma_w = 0.737 \text{ erg/cm}^2$ plus a phonon correction equal to $\hbar s d_m^3 / 48\pi$. This energy is much more sensitive to the choice of cutoff than is the free-surface tension.

Our result for $n_w(z)$ is qualitatively similar to that of Liu, Kalos, and Chester¹⁴ who found $n(z)$ for a gas of hard-sphere bosons between two walls by direct integration of the Schrödinger equation. It is interesting that we find oscillations in the density at a hard wall, in agreement with Ref. 14, but none at a free surface in agreement with Refs. 12 and 13 (although not with Ref. 11). This demonstrates the power and versatility of our theory and suggests that it be applied to other situations such as a realistic wall including van der Waals forces and helium films of finite thickness.

V. SIMPLE MODEL

In this section we present a simple, essentially phenomenological, density-functional theory for ${}^4\text{He}$. The simplicity of the model allows one to perform, with relative ease, a wide variety of calculations. Further, it is the first model to be exactly solvable for the case of a planar free surface. We will here neglect zero-point renormalization. However, since the surface tension derived from the model is of the same order of magnitude as that for real ${}^4\text{He}$, this neglect is not expected to destroy the considerable value of the qualitative conclusions to be drawn.

The density functional is obtained from (2.11) by neglecting the interaction term and representing $\epsilon(n)$ as a power series in the density,

$$\epsilon(n) = An^2 + Bn^3 + Cn^4. \quad (5.1)$$

Constant and linear terms do not appear because

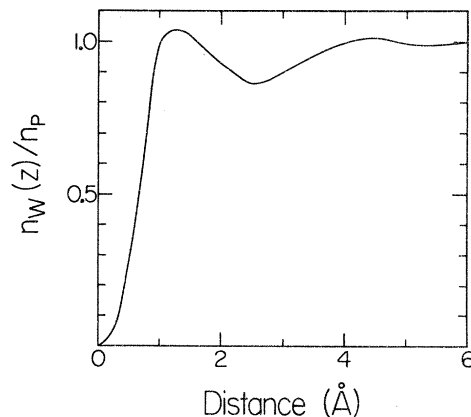


FIG. 10. Density at a hard wall $n_w(z)/n_P$ as a function of the distance from the wall for $P=24.4 \text{ atm}$; the ratio of n_P to the calculated $P=0$ density is 1.25.

we require that both the energy density and chemical potential vanish in the limit of zero density. A similar theory has been presented by Padmore and Cole⁴; however, their theory has the very unphysical feature that $\epsilon(n)$ approaches a non-zero positive constant as $n \rightarrow 0$. The coefficients A , B , and C are fixed by demanding that the energy density, chemical potential, and compressibility be those for real ⁴He at zero temperature and pressure. Consequently,

$$A = (\epsilon_B/n_0)(\frac{1}{2}w - 3), \quad B = (\epsilon_B/n_0^2)(3 - w), \quad (5.2)$$

$$C = (\epsilon_B/2n_0^3)(w - 2),$$

where

$$w \equiv ms^2/\epsilon_B = 3.8. \quad (5.3)$$

Using (5.1), the equation determining the density $\delta E/\delta n(\vec{r}) = \mu$ becomes

$$-\frac{\hbar^2}{2m} \frac{\nabla^2 n^{1/2}(\vec{r})}{n^{1/2}(\vec{r})} + 2An(\vec{r}) + 3Bn^2(\vec{r}) + 4Cn^3(\vec{r}) = \mu. \quad (5.4)$$

We first solve (5.4) for the case of a planar free surface normal to the z axis. The surface is located in the region near $z=0$ and the bulk of the

liquid in the $z > 0$ half space. In this situation, since $n(\vec{r})$ is a function only of z and $\mu = -\epsilon_B$, (5.4) takes the form

$$y''(x) = y(x)[1 + \beta_1 y^2(x) + \beta_2 y^4(x) + \beta_3 y^6(x)], \quad (5.5)$$

in which

$$x = [2m\epsilon_B/\hbar^2]^{1/2} z, \quad y(x) = [n(z)/n_0]^{1/2},$$

$$\beta_1 = w - 6 = -2.2, \quad \beta_2 = 3(3 - w) = -2.4, \quad (5.6)$$

$$\beta_3 = 2(w - 2) = +3.6.$$

Using the conditions $y(-\infty) = 0$ and $y'(-\infty) = 0$, a first integral

$$y'(x) = [y^2(x) + \frac{1}{2}\beta_1 y^4(x) + \frac{1}{3}\beta_2 y^6(x) + \frac{1}{4}\beta_3 y^8(x)]^{1/2} \quad (5.7)$$

of (5.5) is obtained simply by multiplying that equation by $y'(x)$. Using (5.6), this result simplifies to

$$y'(x) = a^{-1/2} y(x)[1 - y^2(x)][y^2(x) + a]^{1/2}, \quad (5.8)$$

where

$$a \equiv 2/(w - 2). \quad (5.9)$$

Equation (5.8) may be directly integrated to yield

$$x = x_0 + \frac{1}{2} \left(\frac{a}{1+a} \right)^{1/2} \ln \left(\frac{2(1+a) + 1 - y^2 + 2[(1+a)(y^2+a)]^{1/2}}{1 - y^2} \right) - \frac{1}{2} \ln \left(\frac{2a + y^2 + 2[a(y^2+a)]^{1/2}}{y^2} \right). \quad (5.10)$$

The constant of integration x_0 determines the position of the surface. The condition $y^2(0) = \frac{1}{2}$ centers the surface at $x=0$ and, using (5.6) and (5.9), yields $x_0 = 0.616$. The result is plotted in Fig. 11. From (5.10), (5.6), and (5.9) one obtains the asymptotic results

$$n(z) \xrightarrow{z \rightarrow -\infty} 4an_0 e^{2x_0} e^{2(2m\epsilon_B/\hbar^2)^{1/2} z}, \quad (5.11)$$

$$n(z) \xrightarrow{z \rightarrow +\infty} n_0 \{1 - 4(1+a) e^{-2[(1+a)/a]^{1/2} x_0} e^{-2(ms^2/\hbar^2)^{1/2} z}\}.$$

The asymptotic behavior far from the bulk is thus governed by the binding energy, whereas the approach to the equilibrium density n_0 upon moving into the liquid is determined by the compressibility.

The surface tension for the present model (neglecting zero-point-motion contributions) may be obtained numerically from (5.10) and (2.17), the result being $\sigma_0 = 0.111$ erg/cm². Another quantity of current interest is the distance between the position z_t of the surface of tension, defined by³⁴

$$z_t = \int_{-\infty}^{\infty} z[\epsilon(n(z)) - \mu n(z)] dz \Big/ \int_{-\infty}^{\infty} [\epsilon(n(z)) - \mu n(z)] dz \quad (5.12)$$

and the position z_0 assigning zero mass to the sur-

face,³⁵ given implicitly by

$$\lim_{L \rightarrow \infty} \left[\int_{-\infty}^L n(z) dz \Big/ \int_{z_0}^L n_0 dz \right] = 1. \quad (5.13)$$

Our numerical result is

$$\delta \equiv z_0 - z_t = -0.337 \text{ \AA}, \quad (5.14)$$

which has the same sign and order of magnitude as that used by Edwards *et al.*³⁶ in recent determinations of the ripplon spectrum in ⁴He from fits to

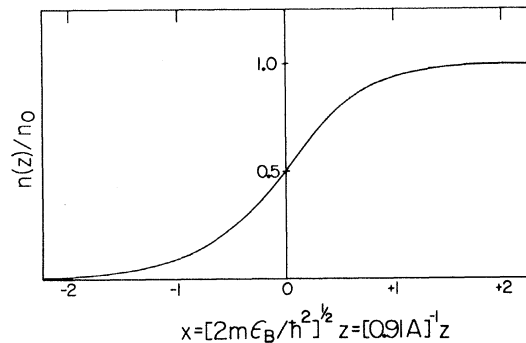


FIG. 11. Reduced density $n(z)/n_0$ vs the dimensionless length $x = [2m\epsilon_B/\hbar^2]^{1/2} z = [0.91 \text{ \AA}]^{-1} z$ for the planar surface case, within the model of Sec. V.

surface-entropy data. The Gibbs surface-mass density is defined as $mm_0\delta$.

Another simple application of the model is a calculation of the ${}^4\text{He}$ density profile near a line vortex. If $\vec{v}(\vec{r})$ is the velocity field associated with the vortex, the equations to be solved are^{18,25}

$$\frac{m\vec{v}^2(\vec{r})}{2} + \frac{\delta E}{\delta n(\vec{r})} = -\epsilon_B, \quad (5.15a)$$

$$\vec{\nabla} \cdot [n(\vec{r})\vec{v}(\vec{r})] = 0. \quad (5.15b)$$

Since $\vec{\nabla}n(\vec{r}) \cdot \vec{v}(\vec{r}) = 0$ in the geometry of interest, (5.15b) becomes $n(\vec{r})\vec{\nabla} \cdot \vec{v}(\vec{r}) = 0$, which has the solution

$$v(r) = \frac{\kappa}{2\pi r} \hat{e}_\theta, \quad (5.16)$$

where r and θ are the radial and angular variables in a cylindrical coordinate system, \hat{e}_θ is a unit vector in the θ direction, and κ is the circulation. For a single quantum of circulation $\kappa = 2\pi\hbar/m$. Using this value for κ , the model density functional, and (5.16) Eq. (5.15a) may be put in the form

$$\begin{aligned} \frac{1}{y} \frac{d}{dy} y \frac{df(y)}{dy} - \frac{f(y)}{y^2} \\ = f(y)[1 + \beta_1 f^2(y) + \beta_2 f^4(y) + \beta_3 f^6(y)], \end{aligned} \quad (5.17)$$

in which $y \equiv (2m\epsilon_B/\hbar^2)^{1/2}r$, $f(y) \equiv (n(r)/n_0)^{1/2}$, and the β_i 's are given in (5.6). The boundary conditions on (5.17) are $f(\infty) = 1$, in order that the density approach the bulk value far from the vortex, and $f(0) = 0$, so that the kinetic energy per unit vortex length be finite [see (5.16)]. It is easy to verify that the latter restriction implies $f(y) \sim y$ for small y . Using these boundary conditions, numerical integration of (5.17) yields the density profile shown in Fig. 12.

As a final application of this simple model we consider the spherical helium droplet. For this situation, (5.4) becomes

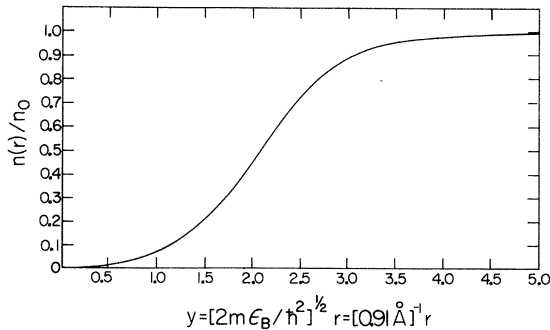


FIG. 12. Reduced density $n(r)/n_0$ vs the dimensionless radial coordinate $y = [2m\epsilon_B/\hbar^2]^{1/2}r = [0.91 \text{ \AA}]^{-1}r$ near a line vortex, calculated within the model of Sec. V.

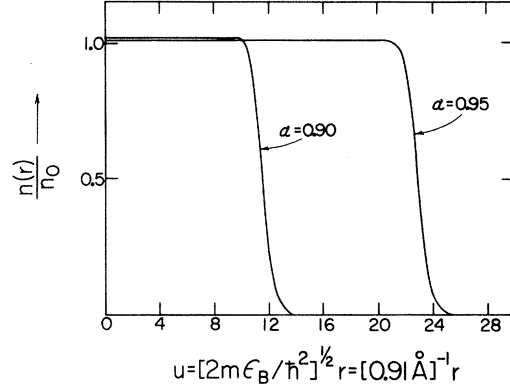


FIG. 13. Reduced density $n(r)/n_0$ vs the dimensionless radial coordinate $u = [2m\epsilon_B/\hbar^2]^{1/2}r = [0.91 \text{ \AA}]^{-1}r$ for spherical droplets with chemical potentials $\mu = 0.90\epsilon_B$ and $\epsilon = -0.95\epsilon_B$. These results are obtained for the model problem of Sec. V.

$$\begin{aligned} \frac{1}{u^2} \frac{d}{du} \left(u^2 \frac{dg(u)}{du} \right) \\ = g(u)[\alpha + \beta_1 g^2(u) + \beta_2 g^4(u) + \beta_3 g^6(u)], \end{aligned} \quad (5.18)$$

in which

$$g(u) = [n(r)/n_0]^{1/2}, \quad u = [2m\epsilon_B/\hbar^2]^{1/2}r, \quad \alpha \equiv -\mu/\epsilon_B, \quad (5.19)$$

and r is the radial coordinate. The dimensionless chemical potential α differs from unity since we are considering a finite system. The size of the droplet is determined by $\alpha < 1$, the limiting value $\alpha = 1$ being achieved for a droplet of infinite size. Far from the bulk of the droplet $g(u) \sim e^{-\alpha^{1/2}u}/u$ and, for reasons of symmetry, $g'(0) = 0$. Imposing these conditions, we have numerically integrated (5.18).³⁷ For $\alpha = 0.90$ and 0.95 , the resultant density profiles $g(y)$ are depicted in Fig. 13.

Order-of-magnitude estimates of the curvature dependences of the surface tension and the distance δ between the surface for real ${}^4\text{He}$ can be obtained from our solutions $g(y)$. To calculate these quantities we use the quasithermodynamic theory of Ono and Kondo.³⁸ In the present model, the total energy density is

$$\epsilon_{\text{tot}}(r) = \frac{\hbar^2}{2m} \left(\frac{dn^{1/2}(r)}{dr} \right)^2 + \epsilon(n(r)). \quad (5.20)$$

Defining the tangential pressure (diagonal component of the stress tensor in the direction parallel to the surface) by

$$p_T(r) = \mu n(r) - \epsilon_{\text{tot}}(r), \quad (5.21)$$

we have

$$E - \mu N = -4\pi \int_0^\infty p_T(r) r^2 dr, \quad (5.22)$$

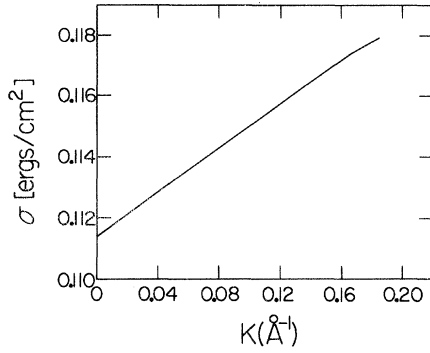


FIG. 14. Surface tension σ vs curvature K for spherical ${}^4\text{He}$ droplets using the model of Sec. V.

where E is the internal energy and N the number of particles in the droplet. The thermodynamic relation

$$E - \mu N = -pV + \sigma A \quad (5.23)$$

then serves to define the surface tension σ in terms of the value of the integral in (5.22), the pressure

$$p = p_T(0) \quad (5.24)$$

far from the surface of the droplet, and the area A and volume V of the droplet. In terms of the droplet radius R ,

$$V = \frac{4}{3}\pi R^3, \quad A = 4\pi R^2. \quad (5.25)$$

The radius R_T of the surface of tension is that value of R for which $d\sigma/dR = 0$, a condition which, since p and $E - \mu N$ are independent of R , yields [from (5.23)] the well-known Laplace equation

$$\sigma = \frac{1}{2}pR_T. \quad (5.26)$$

Combination of (5.22)–(5.26) leads to

$$R_T^3 = \frac{6}{p} \int_0^\infty [\epsilon_{\text{tot}}(r) - \mu n(r)] r^2 dr. \quad (5.27)$$

The zero-mass radius R_0 is defined by

$$R_0^3 = 3 \int_0^\infty n(r) r^2 dr. \quad (5.28)$$

From our solutions to (5.18) and (5.26)–(5.28) we have numerically obtained σ and

$$\delta \equiv R_0 - R_T \quad (5.29)$$

as functions of the droplet curvature

$$K \equiv 2/R_T. \quad (5.30)$$

The results are plotted in Figs. 14 and 15. We also find $(\partial\sigma/\partial K)_{K=0} = 3.7 \times 10^{-2}$ erg/cm and $(\partial\delta/\partial K)_{K=0} = 0.301 \text{ \AA}^2$. The latter derivative is of interest since it is of the same order of magnitude as values used by Edwards *et al.*³⁶ in their fits of ripplon spectra to empirical surface-entropy data.

The former provides, because of its small size, justification of the neglect of curvature dependence of the surface tension in a recent calculation of ripplon damping.³³

VI. DISCUSSION

In applying density-functional theory to a calculation of the properties of the free surface of superfluid ${}^4\text{He}$ we have demonstrated a clear need for modification of the BDF theory in order to include the important effects due to zero-point motion. Further, we have developed a renormalization scheme which self-consistently takes these effects into account. A more sophisticated treatment would incorporate the physics contained within this scheme directly into the original density functional. Further research in this direction is needed.

Our predicted surface width is significantly larger than that obtained in Refs. 12 and 13. As yet, there exist no experimental determinations of the width, but we suggest two possibilities. The first involves measurement of the ellipticity of light scattered elastically at the surface. If light incident at the Brewster angle is polarized at an angle of 45° with respect to the plane of incidence, the ellipticity \mathcal{E} of the scattered light is given by³⁹

$$\mathcal{E} = \frac{k}{\sqrt{2}} \frac{\epsilon - 1}{n_0^2} \int_{-\infty}^{\infty} dz n(z) [n_0 - n(z)], \quad (6.1)$$

where k is the wavenumber of the light and ϵ is the ${}^4\text{He}$ dielectric constant. This result assumes that the wavelength of the light is large compared to the surface width and that the Clausius-Mossotti equation is applicable. It is clear that \mathcal{E} measures a surface width l defined by $l = \int_{-\infty}^{\infty} dz n(z) [n_0 - n(z)] / n_0^2$. A second method for measuring the width involves the elastic scattering of neutrons from the surface. Since the neutron reflectivity R for large angles of incidence is exceedingly small, it would be best to perform measurements near the angle

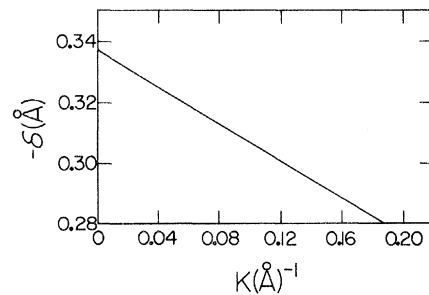


FIG. 15. Distance $\delta = R_0 - R_T$ between the radius R_0 of the zero-mass surface and the radius R_T of the surface of tension, plotted vs the curvature K of spherical ${}^4\text{He}$ droplets. These results pertain to the model discussed in Sec. V.

for critical reflection. In this case one finds that

$$R = R_0 \left(1 - \frac{8k_z(k_z^2 - 4\pi b n_0)^{1/2}}{n_0} \times \int_{-\infty}^{\infty} dz z [n(z) - \theta(z)n_0] \right), \quad (6.2)$$

where R_0 is the reflectivity for a perfectly sharp surface, k_z is the z component of the neutron wave vector, and b is the ^4He -neutron-scattering length.

An interesting result of Sec. IV is the prediction of static density oscillations in ^4He near a hard wall. It is worthwhile to point out that these oscillations may reasonably be expected to persist in the situation where the helium is in contact with a real substrate, next to which several solid ^4He layers are formed⁴⁰ (due to the substrate van der Waals attraction), followed by the liquid. We hope to generalize our formalism to treat this case. Significant structure (in the density) in the neighborhood of this liquid ^4He -solid ^4He boundary could conceivably have an important effect on the Kapitza resistance in the temperature region (1–2 °K) where the effective thermal-phonon wavelengths are comparable to those of the static density oscillations (especially if we note that the characteristic wave number for the energy current is about $3k_B T/\hbar s$ and that the phonons can approach the surface at an angle).

APPENDIX

Here we derive Eqs. (2.26) and (2.28) of the text. While these may be derived⁸ by quantization of the appropriate ideal-fluid hydrodynamic equations, treated as field equations, we have, for present purposes, no need of all the detail contained in such an approach. The mean-square displacement ξ_0^2 can be obtained from the structure factor $S_{\zeta\zeta}(\vec{q}, \omega) \equiv \langle 0 | \xi^\dagger(\vec{q}, \omega) \xi(\vec{q}, \omega) | 0 \rangle$, which in turn is derivable from the retarded ζ - ζ correlation function $\chi_{\zeta\zeta}(\vec{q}, \omega)$; $\chi_{\zeta\zeta}(\vec{q}, \omega)$ is found from the solution of the ideal-fluid hydrodynamic equations in the presence of an external pressure (in Fourier transform) $\delta P_{\text{ext}}(\vec{q}, \omega)$ applied to the exterior surface of the liquid. In fact,

$$\chi_{\zeta\zeta}(\vec{q}, \omega) = \delta\zeta(\vec{q}, \omega) / \delta P_{\text{ext}}(\vec{q}, \omega) \quad (A1)$$

and for zero temperature

$$S_{\zeta\zeta}(\vec{q}, \omega) = 2\hbar \text{Im} \chi_{\zeta\zeta}(\vec{q}, \omega). \quad (A2)$$

The $\chi_{\zeta\zeta}(\vec{q}, \omega)$ is easily calculated along the lines set forth in Sec. III of Ref. 41. One need only alter Eqs. (18b) and (19b) of that reference by setting $\delta U(\vec{r}, t) = 0$ in the former and adding $\delta P_{\text{ext}}(\vec{r}, t)|_{z=0}$ to the right-hand side of the latter. Straightforward calculation then yields, for $\omega > 0$,

$$S_{\zeta\zeta}(\vec{q}, \omega) = \begin{cases} \frac{\kappa \pi \hbar}{\omega \rho} \delta(\omega - \omega_r), & \omega < s q, \\ \frac{2\hbar k_z \omega^2}{\rho(\omega^4 + \omega_z^4)}, & \omega > s q. \end{cases} \quad (A3)$$

At zero temperature $S_{\zeta\zeta}(q, \vec{\omega}) = 0$ for $\omega < 0$. In (A3),

$$\begin{aligned} \kappa &= (q^2 - \omega^2/s^2)^{1/2}, & \omega_r &= (\sigma \kappa q^2/\rho)^{1/2}, \\ k_z &= (\omega^2/s^2 - q^2)^{1/2}, & \omega_z &= (\sigma k_z q^2/\rho)^{1/2}. \end{aligned} \quad (A4)$$

In terms of $S_{\zeta\zeta}(\vec{q}, \omega)$,

$$\xi_0^2 = \int \frac{d^2 q}{(2\pi)^2} \int_0^\infty \frac{d\omega}{2\pi} S_{\zeta\zeta}(q, \vec{\omega}). \quad (A5)$$

Combining (A3)–(A5) gives, after some calculation,

$$\xi_0^2 = [\xi_0^2]^{\text{ripp1on}} + [\xi_0^2]^{\text{phonon}}, \quad (A6)$$

where

$$[\xi_0^2]^{\text{ripp1on}} = \frac{\hbar}{\sqrt{2\pi} \rho s b^2} \int_0^\infty \frac{g^{5/2}(x) dx}{g^2(x) + x^2}, \quad (A7a)$$

$$[\xi_0^2]^{\text{phonon}} = \frac{\hbar}{4\pi^2 \rho s b^2} \int_0^{b^2 q_m^2} I(x) dx. \quad (A7b)$$

In Eqs. (A7),

$$g(x) = -x^2 + x(1+x^2)^{1/2}, \quad b = \sigma/\rho s^2, \quad (A8)$$

$$I(x) = \frac{1}{2} \left[1 + \frac{x^{1/2}}{(1+x)^{3/2}} \ln \left(\frac{(1+x)^{1/2} + x^{1/2}}{(1+x)^{1/2} - x^{1/2}} \right) \right].$$

The term $[\xi_0^2]^{\text{ripp1on}}$ comes from integrating the term with the δ function in (A3). In this case no cutoff is necessary so that the integral in (A7a) is extended to infinity. The remaining term in (A3) gives rise to $[\xi_0^2]^{\text{phonon}}$, for which a cutoff at large wavenumbers q_m is required. The integral in (A7a), done numerically, has the value 0.278; combination of this result with Eqs. (A7) and (A8) yields Eq. (2.26) of the text.

We turn now to the derivation of Eq. (2.28). The ripplon zero-point energy per unit area is clearly

$$\epsilon_{z\text{p}}^{\text{ripp1on}} = \frac{1}{2} \int \frac{d^2 q}{(2\pi)^2} \hbar \omega_{q\kappa} \quad (A9)$$

where the ripplon frequency $\omega_{q\kappa}$ for a compressible fluid is determined by⁴²

$$\omega_{q\kappa}^2 = s^2(q^2 - \kappa^2) = \sigma \kappa q^2/\rho. \quad (A10)$$

Combining (A9) and (A10) leads immediately to the first of equations (2.28).

To derive the second, we solve the hydrodynamic equations⁴² for a slab having thickness L along the z axis and two free surfaces. Consideration of wave solutions of the form $e^{i\vec{q}\cdot\vec{r}} e^{-i\omega t} (e^{ihz} - R e^{-ihz})$, where \vec{q} is perpendicular to the z axis, lead immediately to the conclusions that the allowed wave vectors k are determined by the condition

$$kL - 2 \tan^{-1} [b q^2 k / (q^2 + k^2)] = \pi n, \quad (A11)$$

where $n \geq 1$ is a positive integer and that the frequencies obey $\omega^2 = s^2(q^2 + k^2)$. The wave vectors \vec{q} are determined by periodic boundary conditions. For area A , the phonon zero-point energy of the system is then

$$E_{zp}^{\text{phonon}} = A \int \frac{d^2q}{(2\pi)^2} \sum_{n=1,2,\dots} \frac{\hbar s [q^2 + k^2(n)]^{1/2}}{2}. \quad (\text{A12})$$

For brevity, let $f(n) = \frac{1}{2} \hbar s [q^2 + k^2(n)]$. Assuming that all derivatives of $f(n)$ are zero at $n = \infty$ (i. e., assuming a cutoff wave number), the Euler-MacLaurin formula⁴³ gives

$$\sum_{n=1,2,\dots} f(n) = -\frac{f(0)}{2} + \int_0^\infty f(n) dn - \sum_{\text{odd } r} \frac{B_r}{r+1} \left. \frac{d^r f(n)}{dn^r} \right|_{n=0}. \quad (\text{A13})$$

Here the B_r are Bernoulli numbers. Next, we change to the variable k using the relation [see (A11)]

$$\frac{dn}{dk} = \frac{L}{\pi} \left(1 - \frac{2}{L} \frac{b(1-x^2)(1-2x^2)}{1+b^2 p^2 x^2 (1-x^2)^2} \right), \quad (\text{A14})$$

in which $p^2 = q^2 + k^2$, $k = px$, and $q = p(1-x^2)^{1/2}$. Equation (A13) becomes

$$\sum_{n=1}^\infty f(n) = -\frac{f(0)}{2} + \frac{L}{\pi} \int_0^\infty f(n) \times \left(1 - \frac{2}{L} \frac{b(1-x^2)(1-2x^2)}{1+b^2 p^2 x^2 (1-x^2)^2} \right) dk + O\left(\frac{1}{L}\right). \quad (\text{A15})$$

Insertion of (A15) into (A12) gives, for large L , a term proportional to the volume $V = AL$ plus a term proportional to A . Dividing the latter term by A gives twice (since there are two surfaces) the phonon zero-point surface tension $\sigma_{zp}^{\text{phonon}}$. Consequently,

$$\sigma_{zp}^{\text{phonon}} = -\frac{1}{4} \int \frac{d^2q}{(2\pi)^2} \frac{\hbar s q}{2} - \int \frac{d^3p}{(2\pi)^3} \times \frac{\hbar s p}{2} \frac{b(1-x^2)(1-2x^2)}{1+b^2 p^2 x^2 (1-x^2)^2}. \quad (\text{A16})$$

Straightforward integration using a cutoff wave number q_m yields the second of Eqs. (2.28).

*Research supported by NSF Grant No. GH-31650A-1 and an Ohio State University research grant.

¹P. Hohenberg and W. Kohn, Phys. Rev. **136**, B864 (1964); N. D. Mermin, Phys. Rev. **137**, A1441 (1965).

²An excellent review of this area is given by N. D. Lang, in *Solid State Physics*, edited by H. Ehrenreich, F. Seitz, and D. Turnbull (Academic, New York, 1973), Vol. 28, p. 255.

³A brief report on part of the present work has already appeared. See W. F. Saam and C. Ebner, Phys. Rev. Lett. **34**, 253 (1975).

⁴See, e.g., T. C. Padmore and M. W. Cole, Phys. Rev. A **9**, 802 (1974).

⁵J. W. Negele, Phys. Rev. C **1**, 1260 (1970).

⁶Many of the extant calculations of the free-surface shape for classical liquids may be viewed as density-functional theories. For a review of this area, see C. Croxton, Adv. Phys. **22**, 385 (1973).

⁷J. P. Hernandez, Phys. Rev. A **7**, 1755 (1973).

⁸Details of the quantization of the hydrodynamics for superfluid ⁴He with a free surface are given by W. F. Saam, Phys. Rev. B (to be published).

⁹K. R. Atkins, Can. J. Phys. **31**, 1165 (1953).

¹⁰R. A. Craig [Phys. Rev. B **6**, 1134 (1972)] and J. Schmit and A. A. Lucas [Solid State Commun. **11**, 415 (1972)] obtained large contributions to metallic surface energies due to the zero-point motion of plasmons. Their work has been criticized by P. J. Feibelman [Solid State Commun. **13**, 319 (1973)] and W. Kohn [Solid State Commun. **13**, 323 (1973)], whose most telling point, in our opinion, is that if the plasmon contributions were important, some unexplained mechanism would have to conspire to cancel the equally important contributions obtained by N. D. Lang and W. Kohn [Phys. Rev. B **1**, 4555 (1970)]. A recent systematic discussion of this controversy is given by J. Harris and R. O. Jones [J. Phys. F **4**, 1170 (1974)]. In our

case, neglect of zero-point contributions gives a surface energy, arising from our density functional, which is more than an order of magnitude too small. Further, our procedure self-consistently deals with both zero-point and DF terms, the renormalized DF part comprising about $\frac{2}{3}$ of the final surface energy.

¹¹T. Regge, J. Low Temp. Phys. **9**, 123 (1972).

¹²Y. M. Shih and C.-W. Woo, Phys. Rev. Lett. **30**, 478 (1973).

¹³C. C. Chang and M. Cohen, Phys. Rev. A **8**, 1930 (1973).

¹⁴K. L. Liu, M. H. Kalos, and G. V. Chester, in *Monolayer and Submonolayer Helium Films*, edited by J. G. Daunt and E. Lerner (Plenum, New York, 1973), p. 95.

¹⁵D. O. Edwards, J. R. Eckardt, and F. M. Gasparini, Phys. Rev. A **9**, 2070 (1974).

¹⁶It is possible that the condensate number density should be considered as an additional independent variable here. Our approach assumes that it is not.

¹⁷See, e.g., D. Pines and P. Nozières, *The Theory of Quantum Liquids* (Benjamin, New York, 1966), Vol. 1, Chap. 2.

¹⁸E. P. Gross, Nuovo Cimento **20**, 454 (1961).

¹⁹E. P. Gross, J. Math. Phys. **4**, 195 (1963).

²⁰D. Amit and E. P. Gross, Phys. Rev. **145**, 130 (1966).

²¹The quantum pressure emerges naturally in weak-coupling theories of ⁴He (see Refs. 18–20) but, to our knowledge, the present derivation is the first to extract this term in a general way.

²²R. P. Feynman, Phys. Rev. **94**, 262 (1954).

²³See, e.g., R. Brout and M. Nauenberg, Phys. Rev. **112**, 1451 (1958).

²⁴M. W. Cole, Phys. Rev. A **1**, 1838 (1970).

²⁵L. P. Pitaevski, Zh. Eksp. Teor. Fiz. **40**, 646 (1961) [Sov. Phys.-JETP **13**, 451 (1961)].

²⁶See, e.g., N. D. Mermin, J. Math. Phys. **7**, 1038 (1966).

²⁷The calculation proceeds along the same lines as that for $S_{\xi\xi}$ in the Appendix. The second term on the right-hand side of (2.34) is an approximation to the sum over phonon states valid to a few percent for the range of σ 's involved in our calculation.

²⁸For example, a correction, (due to zero-point "thermal" expansion) given by

$$-\frac{1}{sn_0} \frac{\partial S}{\partial n_0} \langle 0 | \{ \delta n^{\text{op}}[x, y, z + \xi(x, y)] \}^2 n_b[z + \xi(x, y)] | 0 \rangle,$$

where n^{op} is that from the linear theory, will be present. Including this does not alter our results.

²⁹For the same reason, corrections to our adiabatic approximation in (2.32) should have no appreciable effect.

³⁰N. Mihara and R. D. Puff, Phys. Rev. 174, 221 (1968).

³¹N. Mihara, thesis (University of Washington, 1968) (unpublished).

³²The measurements of E. K. Achter and L. Meyer [Phys. Rev. 188, 291 (1969)], taken at $T=0.79$ K at vapor pressure agree quite well with our results for $S_q(n_0)$. B. Mozer, L. A. De Graaf, and B. Le Neindre [Phys. Rev. A 9, 448 (1974)] have measured S_q for several densities. However, it appears that the temperatures used were too high to render detailed comparison with our theory meaningful. This can be seen by comparing their results with those of Achter and

Meyer.

³³W. F. Saam, Phys. Rev. A 8, 1918 (1973).

³⁴See, e.g., R. Defay, I. Prigogine, and A. Bellemans, *Surface Tension and Adsorption* (Wiley, New York, 1966), Chap. 1.

³⁵See, e.g., L. D. Landau and E. M. Lifshitz, *Statistical Physics* (Pergamon, London, 1958), Chap. 15.

³⁶D. O. Edwards, J. R. Eckhardt, and F. M. Gasparini, Phys. Rev. A 9, 2070 (1974).

³⁷All our calculations are for values of α in the range $0.9 \leq \alpha \leq 1.0$. In this range the droplets are stable in that the total energy E is negative.

³⁸S. Ono and S. Kondo, in *Handbuch der Physik*, edited by F. Flügge (Springer, Berlin, 1960), Vol. X, p. 134.

³⁹P. Drude, *Theory of Optics* (Longmans, Green & Co., New York, 1907), p. 292.

⁴⁰See, e.g., J. H. Scholtz, E. O. Mclean, and I. Rudnick, Phys. Rev. Lett. 32, 147 (1974).

⁴¹W. F. Saam, Phys. Rev. A 8, 1048 (1973).

⁴²See, e.g., I. M. Khalatnikov, *An Introduction to the Theory of Superfluidity* (Benjamin, New York, 1965), Chap. 15.

⁴³H. Margenau and G. M. Murphy, *The Mathematics of Physics and Chemistry* (Van Nostrand, Princeton, New Jersey, 1956), p. 474.